

Universality of Interface Trap Generation and Its Impact on I_D Degradation in Strained/Unstrained PMOS Transistors Under NBTI Stress

*A.E. Islam, ¹J. H. Lee, ¹W.-H. Wu, ¹A. Oates, and M.A. Alam

*Email: aeislam@iieee.org, Phone: 765-532-6514, Fax: 765-494-6441

Purdue University, West Lafayette, IN 47907, USA; ¹Taiwan Semiconductor Manufacturing Company, Hsin-Chu, Taiwan

Abstract

Despite extensive use of strained technology, it is still unclear whether NBTI-induced N_{IT} generation in strained transistors is substantially different from that of unstrained ones. Here, we present a comprehensive theory for N_{IT} generation in strained/unstrained transistors and show its universality over a wide range of strain. We further propose that an appropriately designed/optimized transistor might reduce/eliminate NBTI being a concern for CMOS scaling.

1. Introduction

Strain technology has been extensively used over the last three CMOS generations [1]. ESR experiments [2,3] on these transistors confirm that regardless of strain, these transistors are initially characterized by the same type of traps at the Si/SiO₂ interface (N_{IT}). However, it is still unclear whether the mechanism and the rate of NBTI-induced N_{IT} generation (ΔN_{IT}) in these strained devices are, in any way, different from that of unstrained devices. Empirically, even though NBTI activation energy is strain-independent [4-7], reported threshold voltage degradation (ΔV_T) due to ΔN_{IT} , for similar oxide electric field (E_{ox}), are erratic (reported to be slightly decreasing/strain-invariant in [5,8] or increasing with strain in [4,6,7,9-11]). So, the question is: *If the type and mechanism/activation energy of ΔN_{IT} is strain-independent, why does $\Delta N_{IT}@E_{ox}$ (i.e. rate of NBTI-induced ΔN_{IT}) depend on strain?*

In this paper, we answer the aforementioned question through a comprehensive theory of N_{IT} generation (Fig. 1b) for strained/unstrained transistors and demonstrate its validity by interpreting measured ΔN_{IT} for a wide-variety of uniaxial-compressive and biaxial-tensile strained devices. Later, we justify the proposed universality by studying the NBTI field acceleration, NBTI activation energy and hole wave function interaction with N_{IT} (Fig. 4-7). Finally, we explore how ΔN_{IT} translates to I_D degradation (ΔI_D) in strained transistors (Fig. 8), thereby establish the possibility of designing optimized transistors such that it functions indefinitely with no ΔI_D . If realized, this degradation-free transistor would make NBTI less of a concern for future CMOS scaling than it is today.

2. Universal Model for N_{IT} Generation

NBTI-induced ΔN_{IT} has been attributed to the dissociation of SiH bonds at the oxide/substrate interface and subsequent diffusion of H/H₂ species through the oxide and/or poly-Si gate [12-15]. Since oxide/gate materials (i.e., the diffusion medium) are similar, ΔN_{IT} for strained/unstrained transistors

could be different only due to variations in SiH bond dissociation rate (k_f). Ref. [13] envisions a hole-assisted mechanism (Fig. 1b) for SiH bond dissociation and suggests that $k_f \sim p_h * N_0 P_T * \exp(\gamma_T E_{ox}) * \exp(a E_{ox}/kT)$; where, p_h is the hole concentration within inversion layer, N_0 is the SiH bond density, $P_T \sim \exp(-\sqrt{m_{ox}} \phi_{bh})$ is field-independent pre-factor for hole tunneling probability (m_{ox} : oxide effective mass and ϕ_{bh} : barrier height for hole tunneling), $\exp(\gamma_T E_{ox})$ is field-dependent factor for hole tunneling with field acceleration γ_T , and $\exp(a E_{ox}/kT)$ is field-assisted dissociation enhancement factor (a : effective dipole moment and kT : thermal voltage). Thus, NBTI field acceleration, $\gamma = \gamma_T + a/kT$. *Application of strain changes N_0 [2,3] and may also change P_T , γ (through γ_T and/or a). These possibilities are explored below.*

3. ΔN_{IT} for Uniaxial Compressive Strain

To determine $\Delta N_{IT}(t)$, we first measure ΔV_T using measure-stress-measure (MSM) setup [16] for various strained devices having lightly dosed plasma nitrided dielectric (EOT ~ 1.4 nm). Comparison of ΔV_T with N_{IT} 's contribution, $\Delta V_{IT} = \Delta m * E_G$ [17] (Fig. 2) indicates negligible hole-trapping in these devices. To reaffirm this conclusion, we perform on-the-fly $I_{D,lin}$ measurement [18], with 1ms time-zero delay and appropriate mobility correction [16], for both unstrained (Fig. 3a) and strained (Fig. 3b) devices. We find power-law time exponent (n for $\Delta V_T \sim t^n$) of $\sim 1/6$ at wide range of voltages and temperatures and an activation energy of ~ 0.09 eV (Fig. 4a), again suggesting ΔN_{IT} dominates ΔV_T [18] in these devices.

Next, we fit ΔV_T using our field model [13] to determine γ as a function of uniaxial compressive strain (Fig. 4b). We then simulate γ_T (Fig. 4c) using modified WKB approximation [19]. This involves calculation of p_h using self-consistent Schrodinger-Poisson solver [20] and the energy band profile of Fig. 1c, with appropriate effective mass and band-splitting information [21,22]. Invariance of both γ and γ_T with strain indicates negligible variation in $a = kT(\gamma - \gamma_T)$, as well. Hence, *SiH bond dissociation mechanism (i.e. a , γ) is independent of uniaxial compressive strain.*

To further verify the independence of γ_T (i.e. hole wave-function interaction) with uniaxial strain, we study the effective mobility (μ_{eff}) variation in Fig. 5. Empirical mobility model ($\mu_{eff} = \mu_0/[1+\theta(V_G-V_T)^n]$) is used to extract variation in μ_0 ($\Delta\mu_0$) and θ ($\Delta\theta$) parameters using μ_{eff} vs. (V_G-V_T) data obtained before and after NBTI stress (Fig. 5a). We then estimate parameters $P_1 = d(\Delta\mu_0/\mu_{0(0)})/d(\Delta N_{IT})$ and $P_2 = d(\Delta\theta/\theta_0)/d(\Delta N_{IT})$ (Fig. 5b), which provide a reliable signature

of hole wave function interaction with N_{IT} [16]. We find P_1 and P_2 essentially constant (Fig. 5c), thus validating our conclusion that variation of γ_T with strain is negligible.

Given the independence in γ_T and a (hence, γ) with uniaxial compressive strain, the observation that ΔV_T at constant E_{ox} ($\sim V_G - V_T$) decreases with increase in strain (Fig. 6a) can only be explained if *the factor $N_0 P_T$ decreases with compressive strain*. We know that under compressive strain sub-bands with higher confinement effective mass (m_z), i.e. heavy hole (HH) bands, form the top of the valence band. Also, these HH bands are well-separated from the light hole (LH) bands (Fig. 1c). Hence, carrier occupancy in HH bands increases with strain and these carriers face higher ϕ_{bh} , due to higher m_z [1,22]. As a result, P_T decreases with increase in strain, which is consistent with the observed reduction in PMOS gate leakage (at fixed E_{ox}) for these devices (Fig. 6b, also see [1]). Moreover, compressive strain also enhances the lattice mismatch between Si substrate and oxide [2,3], thus increases N_0 . In sum, since $N_0 P_T$ (thus $\Delta V_T @ E_{ox}$ for fixed γ) in our compressively strained transistors decreases with strain, we presume that the decrease in P_T supersedes any increase in N_0 for these devices. Also, there are reports of devices having increased $\Delta V_T @ E_{ox}$ (hence, higher $N_0 P_T$ for same γ) with compressive strain [7,9,10]. This is due to an increase in N_0 by incorporation of enhanced H during SiN deposition. Such increase in N_0 , exceeding the one expected from lattice mismatch [2,3], is probably larger than the decrease in P_T (Fig. 6b), thus increasing $\Delta V_T @ E_{ox}$ with strain for these devices.

4. ΔN_{IT} for Biaxial Tensile Strain

Here, we recompute hole flux into N_{IT} using energy band diagram of Fig. 1d with appropriate effective mass and band-splitting information [23,24]. Extracted γ_T from these calculations shows negligible variation with biaxial strain (Fig. 7a). Since field acceleration (γ) is also independent of biaxial strain [4,6], effective dipole moment for *SiH bond* (i.e. a) should be invariant with biaxial tensile strain, as well as uniaxial compressive strain (as discussed in last section).

Moreover, contrary to compressive strain, tensile strain forces LH to form the top of the valence band (Fig. 1d) [22]. Hence, occupancy in the LH band increases with tensile strain, which enhances gate leakage at fixed E_{ox} [1,6] (due to lower m_z , hence reduced effective hole tunneling barrier for carriers in the LH band) – signifying an increase of P_T in our field model (Fig. 1b). Tensile strain also reduces N_0 due to reduced lattice mismatch between Si substrate and oxide [2,3]. Hence, increased $\Delta V_T @ E_{ox}$, observed in [4,6,11] (Fig. 7b), should have resulted from a dominant increase in P_T with tensile strain, compared to the reduction in N_0 . Thus, *we identify (only) parameter $N_0 P_T$ in our NBTI field model (Fig. 1b) to be strain dependent, which increases (decreases) with tensile (compressive) strain for the transistors under study*.

5. ΔI_D due to ΔN_{IT} in Strained Transistors

Next we study the impact of ΔN_{IT} on $I_{D,lin} \sim \mu_{eff}(V_G - V_T)$ for (uniaxially) strained/unstrained transistors and observe a

reduction in $\Delta I_{D,lin}$ (for similar ΔV_T , or ΔN_{IT}) with an increase in strain (e.g., by decreasing channel length in Fig. 8a \rightarrow Fig. 8b). This might lead one to believe that theory of $\Delta I_{D,lin}$ is different in strained transistors, but it is not. To resolve this, we measure $\Delta \mu_{eff} @ V_G$ and $\Delta \mu_{eff} @ E_{eff}$ (where, E_{eff} is effective electric field [25]) for different devices. We find $\Delta \mu_{eff} @ E_{eff}$ to be always negative (due to enhanced coulomb scattering from ΔN_{IT} [25]), regardless of strain (Fig. 8c). In contrast, $\Delta \mu_{eff} @ V_G$ is negative for lightly-strained transistors, having smaller θ (Fig. 8c, f), and is positive for highly-strained transistors, having larger θ (Fig. 8c, g). This mainly happens due to the decrease in substrate depletion (Q_{dep}) and inversion (Q_{inv}) charges (hence, $E_{eff} \sim Q_{dep} + 1/3 Q_{inv} \sim V_G - V_T$) with increase in N_{IT} at constant V_G (Fig. 8d,e). For strained transistors having larger θ , reduced E_{eff} increases μ_{eff} . Such μ_{eff} improvement can overcome the downward shift of mobility-field curve (i.e., negative $\Delta \mu_{eff} @ E_{eff}$) – resulting positive $\Delta \mu_{eff} @ V_G$ (Fig. 8c, g). On the other hand, in lightly-strained/unstrained transistors, having lower θ , downward shift of mobility-field curve dominates over the effect from E_{eff} reduction – resulting negative $\Delta \mu_{eff} @ V_G$ (Fig. 8c, f). As, $\Delta I_{D,lin} / I_{D,lin0} @ V_G = \Delta \mu_{eff} / \mu_{eff} @ V_G - \Delta V_T / (V_G - V_{T0})$ [16,26], positive $\Delta \mu_{eff} / \mu_{eff} @ V_G$ for highly-strained transistors can easily compensate negative contribution from $-\Delta V_T / (V_G - V_{T0})$, resulting negligible $\Delta I_{D,lin}$ (as well as reduced $\Delta I_{D,sat}$ [26]). Whereas $\Delta \mu_{eff} / \mu_{eff} @ V_G$ is negative in lightly-strained devices, hence no such compensation between $\Delta \mu_{eff}$ and ΔV_T becomes possible. Although self-compensation is here demonstrated for NBTI-related ΔN_{IT} , in principle, this is applicable for hole/electron trapping (during NBTI/PBTI) as well. Hence, it is desirable to design strained transistors to have high θ (for better reliability), as well as high μ_{eff} (for better performance).

6. Conclusion

We have critically examined the impact on NBTI-induced ΔN_{IT} due to uniaxial/biaxial and compressive/tensile strain. Thus, we identify physical model parameters responsible for the observed variations over a wide range of experiments. Finally, we show the possibility of designing transistors for reducing BTI being a concern for CMOS scaling.

Acknowledgement: We acknowledge K. Ahmed of AMAT for the strained samples, Birc Nanotechnology Center for experimental facilities and NCN@Purdue for computational resources used in this work. A.E. Islam also acknowledges his discussions with A.N.M. Zainuddin.

References: [1] Thompson *et al.*, TED, p.1010, 2006. [2] Stesmans *et al.*, APL, p.3038, 2003. [3] Somers *et al.*, JAP, 033703, 2008. [4] Shi *et al.*, IRPS, p.403, 2005. [5] Shickova *et al.*, EDL, p.242, 2007. [6] Irisawa *et al.*, VLSI, p.36, 2007. [7] Rhee *et al.*, IEDM, p.692, 2005. [8] Giusi *et al.*, TED, p.78, 2007. [9] Lu *et al.*, JJAP, p.3064, 2006. [10] Lu *et al.*, JES, H1036, 2007. [11] Liu *et al.*, TED, p.1799, 2007. [12] Alam *et al.*, MR, p.71, 2005. [13] Islam *et al.*, TED, p.2143, 2007. [14] Krishnan *et al.*, APL, 153518, 2006. [15] Grasser *et al.*, IRPS, p.28, 2008. [16] Islam *et al.*, IRPS, p.87, 2008. [17] Ang *et al.*, TDMR, p.22, 2008. [18] Mahapatra *et al.*, IRPS, p.1, 2007. [19] Register *et al.*, APL, p.457, 1999. [20] Islam *et al.*, TED, p.1143, 2008. [21] Uchida *et al.*, IEDM, p.129, 2005. [22] Sun *et al.*, JAP, 104503, 2007. [23] Nayfeh *et al.*, TED, p.2069, 2004. [24] Singh *et al.*, JAP, 4264, 1998. [25] Takagi *et al.*, TED, p.2357, 1994. [26] Islam *et al.*, APL, 173504, 2008.

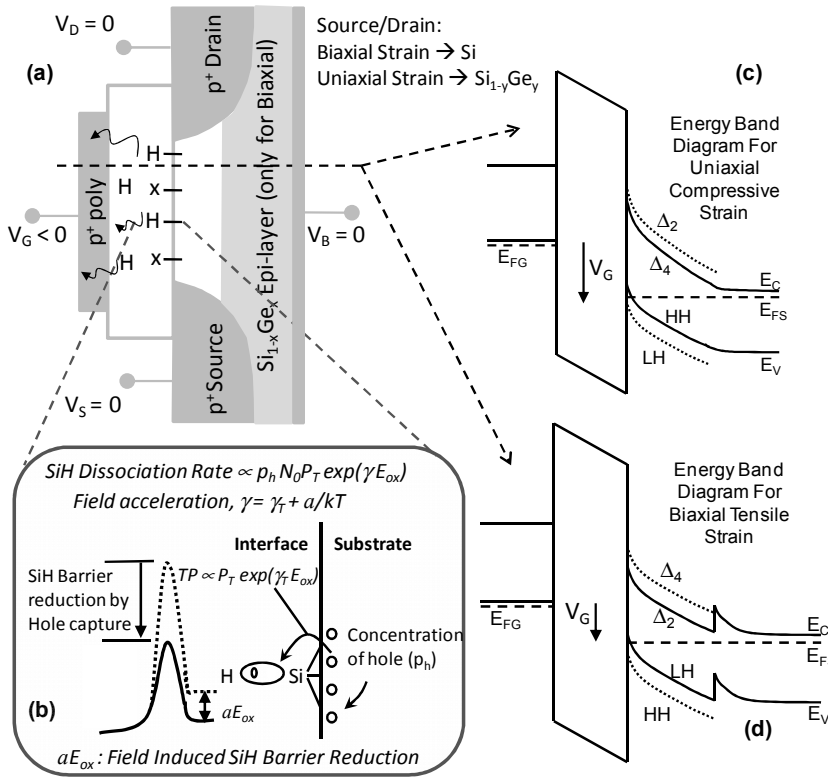


Fig. 1: Universal view of N_{IT} generation (ΔN_{IT}) under NBTI stress in strained/ unstrained devices. **(a)** Schematic of PMOS, showing the application of uniaxial compressive strain using $Si_{1-y}Ge_y$ Source/Drain or biaxial tensile strain using $Si_{1-x}Ge_x$ epi-layer. **(b)** Dissociation mechanism for SiH bond. **(c)** Band diagram during NBTI stress, along the transverse direction, for uniaxially strained device shows the strain induced splitting of electron valleys (Δ_2 and Δ_4) and hole valleys (LH and HH). **(d)** Band diagram for biaxially strained device shows an extra band discontinuity at the strained-Si/ $Si_{1-x}Ge_x$ interface [23].

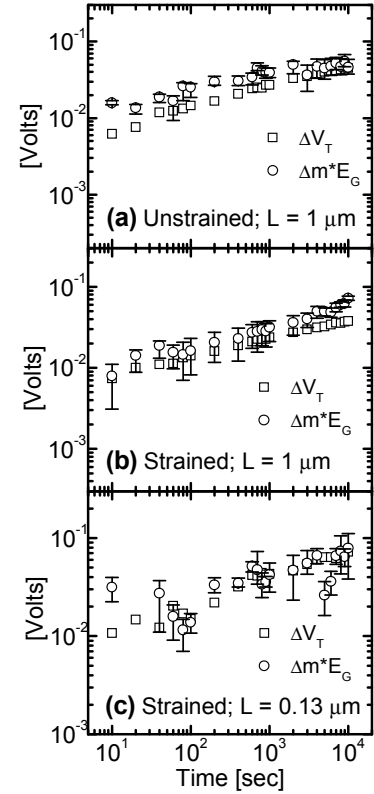


Fig. 2: Comparison of ΔV_T and body-effect coefficient degradation (Δm) indicates negligible hole trapping in the uniaxial devices under study. Here, $\Delta m^* E_G$ indicates N_{IT} 's contribution to ΔV_T , assuming uniform trap generation within the Si bandgap ($E_G \sim 1.1$ eV). Presence of hole trapping is expected to make $\Delta m^* E_G < \Delta V_T$ [17], which is not observed here.

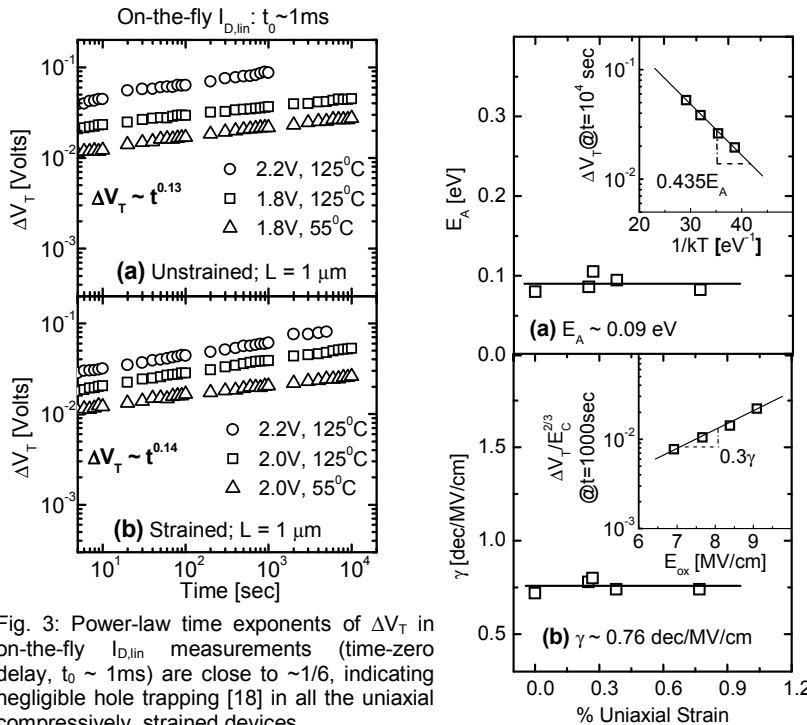


Fig. 3: Power-law time exponents of ΔV_T in on-the-fly $I_{D,lin}$ measurements (time-zero delay, $t_0 \sim 1$ ms) are close to $\sim 1/6$, indicating negligible hole trapping [18] in all the uniaxial compressively strained devices.

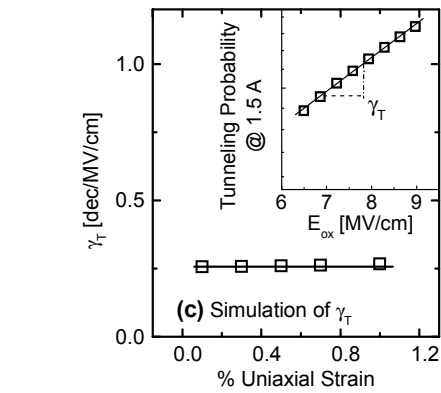


Fig. 4: Uniaxial compressive strain causes: **(a)** Negligible change in NBTI activation energy ($E_A \sim 0.09$ eV), thus indicating similar diffusing species, as well as negligible hole trapping [18]; **(b)** Negligible variation for field acceleration (γ); **(c)** Invariance for simulated γ_T , calculated from tunnel prob. @1.5A (SiH bond length) away from the MOS channel using modified WKB [19]. Thus $a = kT(\gamma - \gamma_T)$ should also be invariant with uniaxial compressive strain. Here, Fig. 4c uses the energy band profile of Fig. 1c, with appropriate information related to effective mass and band-splitting [21,22]; whereas insets show the calculation procedure for E_A , γ , and γ_T .

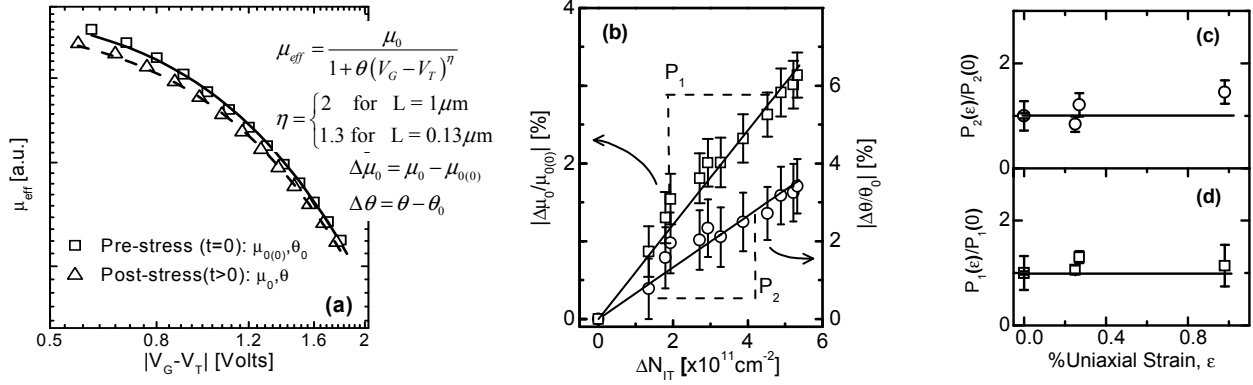


Fig. 5: (a) Generation of N_{IT} decreases effective mobility (μ_{eff}) at fixed $(V_G - V_T)$. We fit μ_{eff} vs. $(V_G - V_T)$ using well-known empirical mobility expression to estimate μ_0 and θ at different stress intervals. Degradation in μ_0 ($\Delta\mu_0$) and θ ($\Delta\theta$) are thus estimated by comparing with their pre-stress values ($\mu_{0(0)}$ and θ_0). (b) $\Delta\mu_0$ and $\Delta\theta$ correlates well with ΔN_{IT} . The slopes of these correlations give P_1 , P_2 , which are signatures of hole wavefunction interaction with N_{IT} [16]. (c) Variation of P_1 and P_2 are independent of uniaxial compressive strain, within the error margin of estimation, which is an independent signature of the invariance in wavefunction interaction (γ_T) with strain.

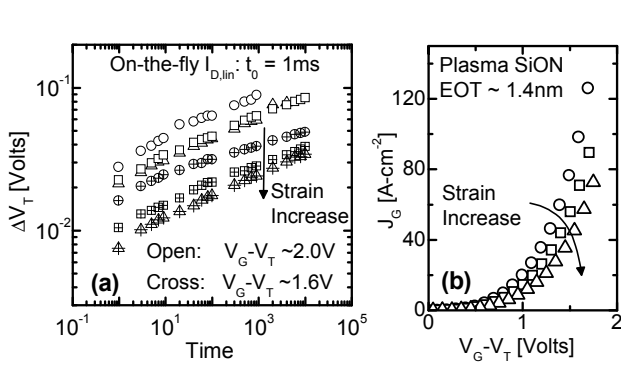


Fig. 6: Though uniaxial compressive strain does not alter field acceleration (Fig. 4, 5), (a) it decreases ΔV_T , measured at similar electric field (or, $V_G - V_T$). This is shown here with three different strained devices, measured using on-the-fly $I_{D,\text{lin}}$ ($t_0 \sim 1\text{ms}$) at two different $V_G - V_T$. Decrease in ΔV_T with strain, for similar γ , implies decrease in $N_0 P_T$ for Fig. 1b. Similarly, (b) decrease in γ , leakage (at same $V_G - V_T$) for similar devices signifies a reduction in P_T , which should be dominating over any increase in N_0 [2,3] to give reduced $N_0 P_T$ with increase in compressive strain.

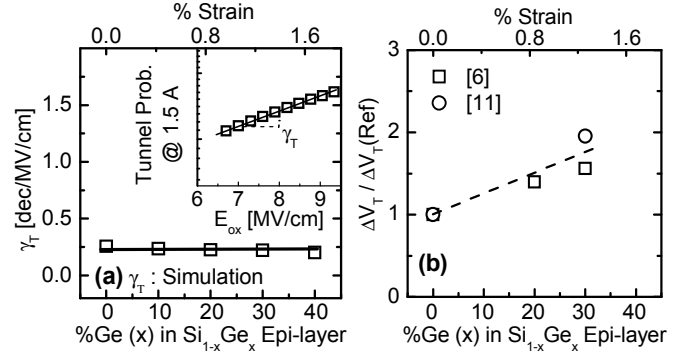


Fig. 7: Biaxial tensile strain results: (a) Invariance for simulated γ_T , calculated from (inset) tunnel prob. @ 1.5Å away from the channel using modified WKB [19]; (b) Increase in ΔV_T (with respect to that for unstrained devices, measured at similar electric field); line is guide to eye only. As, γ is also strain independent [4,6], $a = kT(\gamma - \gamma_T)$ should also be invariant with biaxial tensile strain. Here, Fig. 7a uses the energy band profile of Fig. 1d, with appropriate information related to effective mass and band-splitting [23,24].

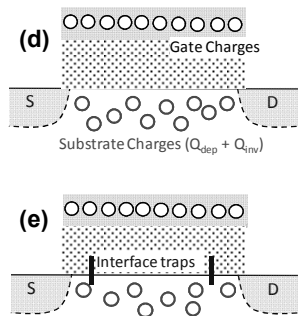
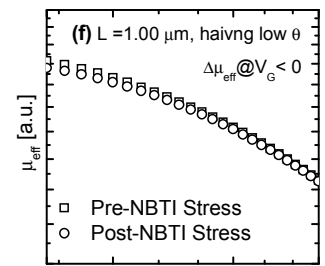
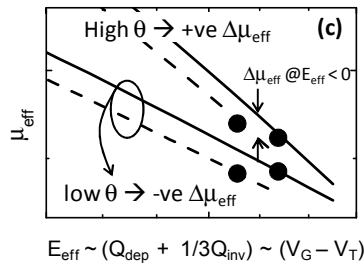
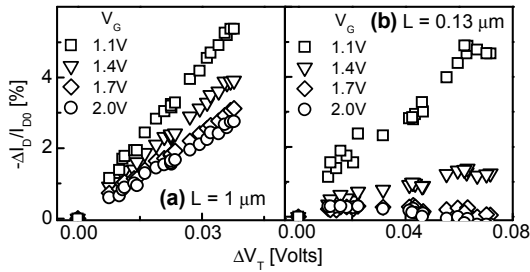


Fig. 8: For similar ΔV_T , $|\Delta I_{D,\text{lin}}|$ decreases with increase in strain. This is evident in (a, b), where uniaxial compressive strain is increased by decreasing channel length. Reduced $|\Delta I_{D,\text{lin}}|$ results from μ_{eff} increase (under NBTI stress at constant V_G) in devices having high θ (c, g) or increased strain [26], compared to the conventional μ_{eff} decrease in devices with low θ (c, f) or reduced strain. **Why μ_{eff} decreases/increases:** Increase in N_{IT} , during constant V_G stress, reduces the amount of substrate charge (d) \rightarrow (e) or E_{eff} , as well as, $\mu_{\text{eff}} @ E_{\text{eff}}$ (c, Fig. 5a). Thus for low θ , μ_{eff} reduction due to shift of $\mu_{\text{eff}} @ E_{\text{eff}}$ curve dominates over the μ_{eff} improvement due to E_{eff} reduction (c), resulting an overall decrease in $\mu_{\text{eff}} @ V_G$ (f). Whereas, for devices having higher θ , μ_{eff} improvement coming from E_{eff} reduction dominates (c), which results an overall increase in $\mu_{\text{eff}} @ V_G$ (g).

